Small-Angle X-ray Diffraction of Muscle Using Undulator Radiation from the Tristan Main Ring at KEK†

Naoto Yagi,[a] Katsuzo Wakabayashi,[b]* Hiroyuki Iwamoto,[c] Keisuke Horiuti,[d] Iwao Kojima,[b] Thomas C. Irving,[e] Yasunori Takezawa,[b] Yasunobu Sugimoto,[b] Syunei Iwamoto,[b] Toshikazu Majima,[f] Yoshiyuki Amemiya[g] and Masami Ando[g]

[a]Department of Pharmacology, Tohoku University School of Medicine, Sendai, Miyagi 980-77, Japan, [b]Department of Biophysical Engineering, Faculty of Engineering Science, Osaka University, Toyonaka, Osaka 560, Japan, [c]Department of Physiology, School of Medicine, Teikyo University, Itabashi-ku, Tokyo 173, Japan, [d]Department of Physiology, Oita Medical University, Hasama, Oita 879-55, Japan, [e]Department of Biological, Chemical and Physical Sciences, Illinois Institute of Technology, Chicago, Illinois 60616, USA, [f]Supermolecular Science Section, Electrotechnical Laboratory, Tsukuba, Ibaraki 305, Japan, and [g]Photon Factory, National Laboratory for High Energy Physics, Tsukuba, Ibaraki 305, Japan

Time-resolved X-ray diffraction of muscle has demanded ever-increasing flux into small sample volumes with low beam divergence. Results are reported of static and time-resolved small-angle X-ray diffraction studies on muscle fibers using a hard X-ray undulator installed in the Tristan main ring at KEK, Tsukuba, Japan, as an innovative source of synchrotron radiation more intense and better collimated than that available with the Photon Factory bending-magnet beamline. Static studies used the low divergence of the source to obtain detailed high-quality diffraction patterns of stable muscle states. The diffraction patterns from live skeletal muscles showed the numerous (over 100) meridional reflections. The well collimated beam from the undulator made it possible to clearly resolve, with an angular resolution of ca 700 nm, the closely spaced diffraction peaks arising from the two halves of the thick filaments centred on the M lines in a sarcomere; in addition, the diffraction peaks from the thin filaments on opposite sides of the Z bands could be resolved with an angular resolution of ca 1000 nm. The detailed structure of the meridional pattern defines the nature of the molecular packing in the thick and thin filaments. Time-resolved experiments using a focusing mirror aimed to prove cross-bridge states in striated muscle fibers by collecting X-ray diffraction data at a 0.185 ms time resolution from sinusoidally oscillating chemically skinned rabbit muscle fibers during active contraction and in rigor. When sinusoidal length changes at 500 Hz with a peak-to-peak amplitude of 0.6% of the muscle length were applied to a small fiber bundle, the tension showed a simple elastic response during the length oscillation. In the active muscle the intensity of the 14.5 nm myosin-based meridional reflection changed out of phase with the tension change during the oscillating length change. In contrast, in the rigor muscle it occurred in phase with the tension change. The high time-resolved experiments provide an insight into the coupling between conformational changes and force generation of the actomyosin cross-bridges. These studies provide a preview of the expected gains for muscle studies from the more widespread use of undulator radiation at third-generation synchrotron sources.

1. Introduction

The modern concept of the mechanism of muscle contraction is based on structural, mechanical and biochemical studies, all indicating that relative sliding between the two types of filaments in the sarcomere (the functional and structural repeating unit along the longitudinal axis of the striated muscle) depends on cyclic ATPase-coupled cross-bridge interactions between myosin heads on the thick filaments and actin in the thin filaments (Huxley, 1974). The exact nature of the force-generating myosin–actin interaction, driven by a hydrolysis of ATP (adenosine

† Transposable Ring Intersecting Storage Accelerator in Nippon (Tristan), at the National Laboratory for High Energy Physics, Tsukuba, Japan (KEK).

triphosphate), remains unclear (Cooke, 1990). Fiber diffraction of muscle has a key role in such studies because of its ability to investigate muscle structures under intact physiological conditions, in fact even in the living state. Furthermore, it has the ability to detect global changes in sarcomere structure at the physiologically relevant millisecond and sub-millisecond timescale.

Small-angle X-ray diffraction of muscle makes unusually high demands on X-ray sources and optics (Huxley & Brown, 1967). Muscles diffract relatively weakly, have many components with similar long spacings, and the changes of physiological states in muscle and the accompanying structural changes occur on a timescale of milliseconds or a few hundreds of microseconds. The lack of X-ray flux necessary to resolve these motions motivated very fast biological experiments using synchrotron radiation (Rosenbaum, Holmes & Witz, 1971; Holmes, 1974), which in turn helped provide the impetus for the construction of second-generation dedicated synchrotron sources with specialized small-angle beamlines (Hamburg EMBL X33, Daresbury 2.1 and 16.1, Photon Factory BL15A).

The major impediment to progress is still the lack of flux. Most synchrotron small-angle diffractometers that have been used for muscle studies to date are on bending-magnet beamlines. Beamline 15A at the Photon Factory has been particularly productive in terms of scientific output but delivered a maximum flux of the order of 8×10^{10} photons s^{-1} into a sample size of the order of 3×2 mm (Amemiya et al., 1983; Wakabayashi & Amemiya, 1990). Smaller beams for smaller samples, achieved by slitting down, contain correspondingly less flux. Time-resolved X-ray patterns have been restricted to only the stronger features of the diffraction pattern, primarily from large whole-muscle specimens. Unfortunately, it is not possible to perform adequate mechanical experiments on the whole muscle and large fiber bundles. State-of-the-art work is performed with single muscle fibers and even myofibrils. Some of the reasons for excluding larger preparations are the inevitable fiber-to-fiber variation, the difficulty of synchronizing and ensuring uniformity of contraction, limitations imposed by diffusion rates of substrates and products, and the difficulty of controlling sarcomere length and force which are necessary to have interpretable results. The beam size from wiggler sources such as the F-1 station at CHESS (Irving & Huxley, 1994) is too large [0.4 mm (V) $\times$ 3 mm (H) at the focus of 2 m] to be used effectively for these studies, although its flux is more than one order of magnitude higher than that from bending-magnet beamlines.

The Tristan Super Light Facility at KEK proposed in the Tristan Super Light Facility Conceptual Design Report (1992) would have been a third-generation light source based on the existing Tristan main ring. The Tristan main ring synchrotron has a circumference of 3018 m, which is the largest among those that have been used as a storage ring, ensuring low emittance. However, because of the decision to build a B factory instead of a synchrotron light facility, the Tristan main ring was only available for

synchrotron radiation experiments for a six-month period in the latter half of 1995, half of which was spent on installing an undulator and monochromators. The remaining three-month period was divided among several applications (Ando & Ohsumi, 1996).

Here we report the results of two small-angle X-ray diffraction experiments on muscle fibers using an undulator inserted in the Tristan main ring as an innovative source of intense and well collimated synchrotron radiation. One experiment was performed to study the structures of the thick and thin filaments in the sarcomere from their X-ray diffraction recorded on a storage-phosphor area detector (an imaging plate). The other experiments aimed to probe cross-bridge states in a striated muscle by collecting one-dimensional time-resolved X-ray diffraction data from chemically skinned rabbit muscle fibers using a rotating-drum imaging-plate system. In these experiments, a sinusoidal length oscillation was applied to the muscle during active contraction and in rigor. Comparison of the time courses of intensity changes of the myosin-based 14.5 nm meridional reflection could be expected to yield insights into the mechanism and kinetics of muscle contraction.

2. Machine characteristics

The Tristan main ring (3018 m in circumference) was used in a dedicated synchrotron radiation operating mode between October and December of 1995 (Kamada et al., 1995). The muscle experiments were performed during this period. The ring energy was set to 8.0 GeV. Beam currents were ca 1–8 mA (in static measurements) and ca 15 mA (in time-resolved measurements) using either 8 or 32 bunches. A 5.4 m undulator was constructed using a modular design with a period of 4.5 cm (λ_u) $\times$ 40 poles (Yamamoto, Shioya, Kitamura & Tsuchiya, 1995). The horizontal emittance of an 8.5 keV beam from this device was calculated to be 5 nm rad so that the expected beam size would be ca 1.7 (V) $\times$ 6 mm (H) at 100 m from the source with a flux of the order of 1×10^{13} photons s^{-1} at 10 mA. The practical machine parameters and the performance of the beamline will be reported elsewhere.

3. Optics and beamline design

The beamline layout for the present experiments is shown in Fig. 1. The first cryogenically cooled Si (220) crystal (Mori et al., 1995) is located ca 87 m from the source. The second Si (220) crystal of the double-crystal monochromator design was located 5 m further from the source and 4.5 m down. This large offset resulted in a very low background of scattered synchrotron and bremsstrahlung radiation. There was no evidence for thermal degradation of beam intensity, showing that cooling of the first monochromator was adequate. The crystals were adjusted to pass the first harmonic of the undulator beam (8.4 keV). Two optics were used depending on the purpose of the experiments. The

specimen-to-detector (imaging plate) distance was *ca* 2 m in both cases.

For static measurements, no focusing optics were employed (Fig. 1*a*). Two pairs of remotely adjustable vertical and horizontal slits, one just behind the second crystal, the other just before the sample 4.5 m downstream, were used. The first pair of slits limited the beam size to 0.14 (V) × 0.57 mm (H). The second pair were used as guard slits to reduce parasitic scatter from the edges of the first pair of slits. The beam size after the second slits was 0.16 × 0.60 mm, showing that the vertical beam size increased by only 0.02 mm over the travelling distance of 4.5 m. The flux was *ca* 5 × 10^8 photons s^{-1} at a ring current of 5 mA. In most experiments the two crystals were slightly misaligned so that the second harmonic of the undulator

spectrum was not passed. When the crystals were better aligned, the second harmonic, which had an intensity $\sim 5\%$ of the fundamental, was observed. Diffraction from this harmonic was evident in some diffraction patterns but it did not seriously hamper the interpretation because its position and intensity were predictable. Diffraction patterns were recorded on an imaging plate which was scanned with a 100 μm pixel size using a BAS 2000 scanner (Fuji Film, Tokyo, Japan).

In the time-resolved experiment a 20 cm-long platinum-coated cylindrically bent glass mirror was inserted horizontally at approximately 95 m from the source and 2 m upstream of the sample position (Fig. 1*b*). The bender was a conventional four-point bending mechanism of the Franks-type (Franks, 1958). The mirror was able to intercept
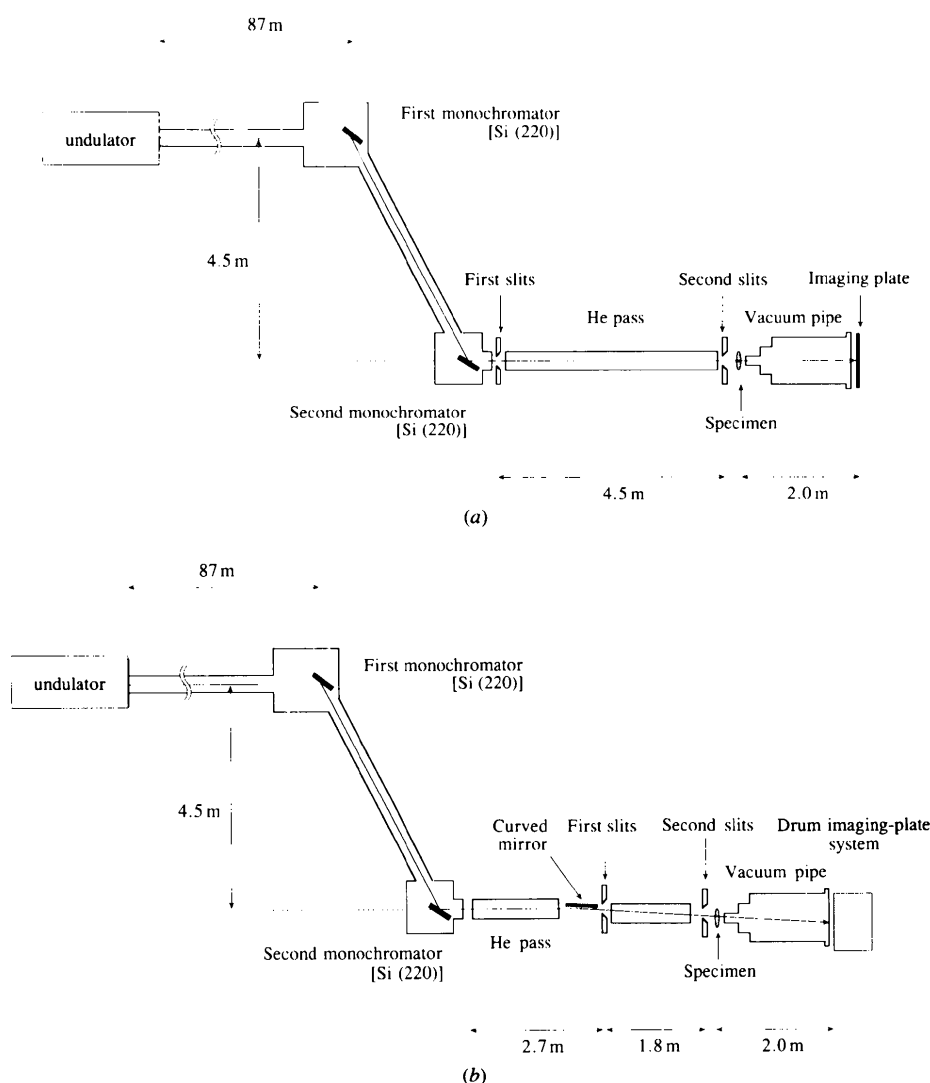
Figure 1
The beamline layout for the diffraction experiments on muscle. (*a*) For the high-spatial-resolution measurements and (*b*) for time-resolved measurements. The crystals were adjusted to pass the first harmonic of the undulator beam (8.4 keV). The first monochromator crystal was cryogenically cooled by liquid nitrogen. The first monochromator box and the bellows pipe connecting it was evacuated and the second monochromator box was filled with He gas. In (*b*) a 20 cm-long platinum-coated bent glass mirror is inserted at approximately 95 m from the source and 1.8 m upstream of the specimen position. The mirror was used to focus the X-ray beam vertically to 0.3 mm at the specimen. The pipe behind the specimen was evacuated by a rotary pump.

ca 40% of the beam and made it focus vertically to a line *ca* 0.3 mm at the specimen position. There was no detectable effect of higher-order harmonics from the undulator with this arrangement. The first pair of slits were placed just behind the mirror, collimating the beam to 0.3 (V) × 2.0 mm (H) on the specimen containing a flux of *ca* 1×10^{11} photons s^{-1} at 15 mA. This flux is one order of magnitude higher flux than that for a similarly sized beam from the Photon Factory BL15A bending-magnet line (Wakabayashi & Amemiya, 1990; Yagi, Takemori & Watanabe, 1993). One-dimensional streak patterns were recorded using the rotating-drum imaging-plate system described below.

4. Results and discussion

4.1. *Static experiments on muscle*

Fig. 2 shows diffraction patterns taken from a frog (*Rana catesbeiana*) live sartorius whole muscle resting in a Ringer solution at room temperature. The exposure was 30 min on an imaging plate with a ring current of *ca* 4 mA. The longitudinal axis of the muscle was oriented vertically and the sample was continuously moved slowly during the exposure to avoid radiation damage. The small beam size ensured sharp reflection peaks, making patterns with high spatial resolution in both meridional and equatorial directions. The patterns also have high contrast because the background is very low. This is mainly due to the simplicity of the optics: there is no focusing element that would tend to cause higher background due to parasitic scattering.

The most notable feature of the diffraction patterns in Fig. 2 is a number of fine intensity peaks (over 100) along the meridian (the central vertical axis of the pattern) in the 0.015–0.25 nm^{-1} region. Fig. 3 depicts the intensity tracings on the meridian after multiplication by the square of the axial coordinate for illustration purposes. These fine peaks, which have a peak-to-peak separation of 700–1000 nm, arise from the sampling (interference effects)
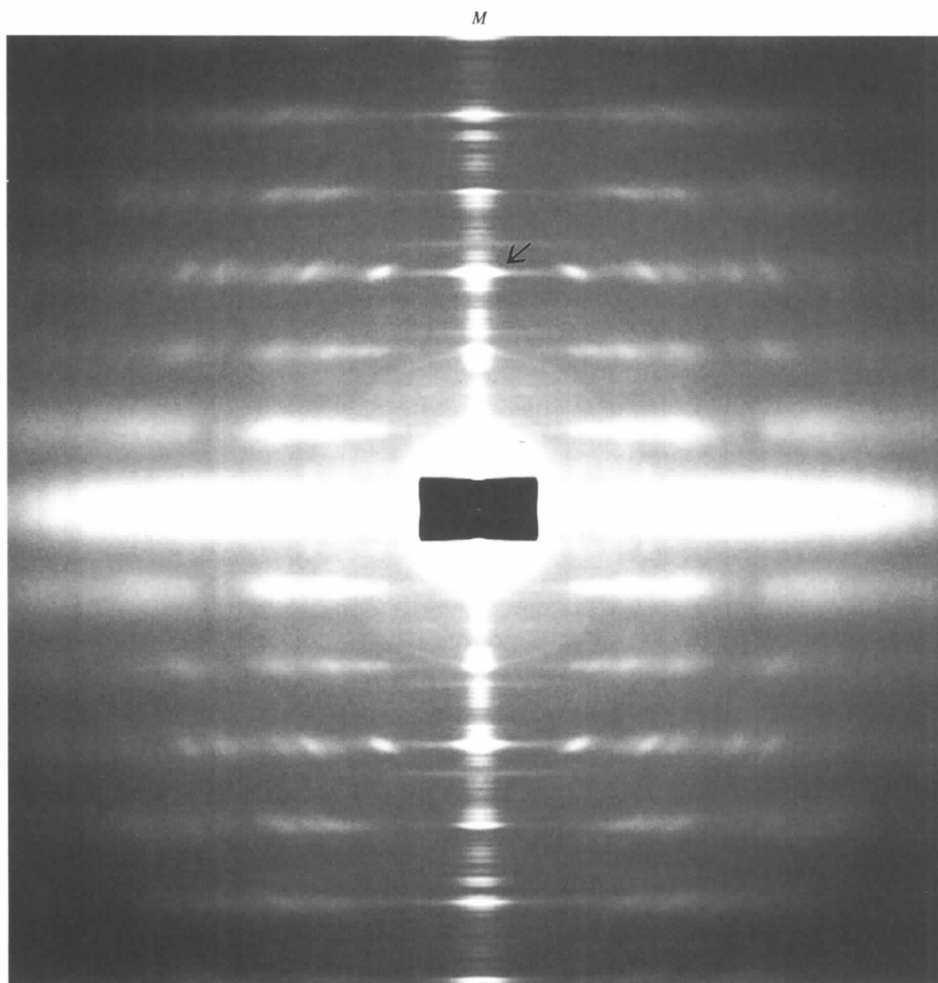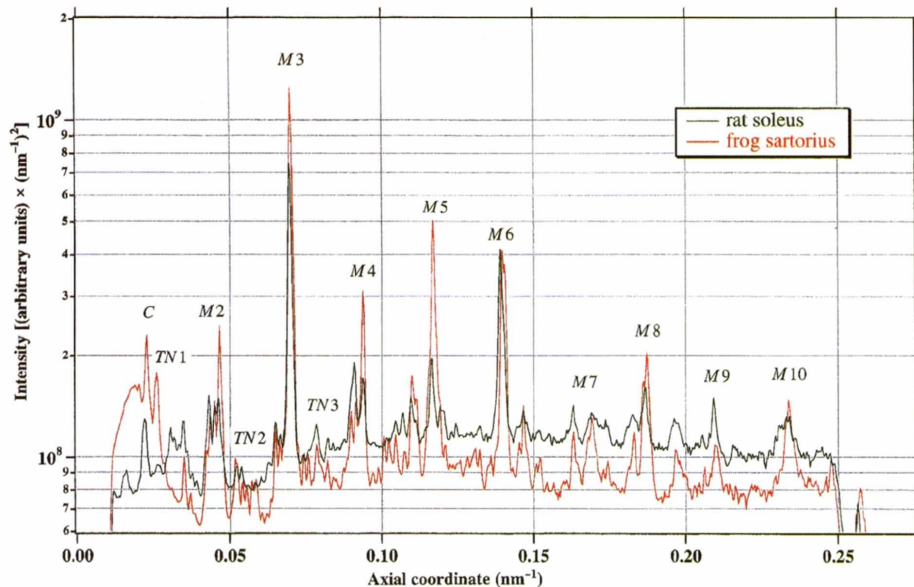

Figure 2
An example of X-ray diffraction patterns taken from frog skeletal muscles in the living relaxed state at room temperature. The pattern was recorded on an imaging plate in an exposure time of 30 min at a camera length of 2 m with a ring current of 4 mA. The fiber axis of the muscle is vertical. The size of the first slit in Fig. 1(*a*) was collimated to 0.14 (V) × 0.57 mm (H). *M* is the meridional axis, *E* is the equator. An arrow indicates the 14.3 nm thick-filament-based meridional reflection. In an active state or rigor state the spacing of this reflection changes to 14.5 nm.

by the long-range periodicities of the transform of the mass projection on the fiber axis. Because the sampling effect from the sarcomere repeat has completely decayed away in this region (Bordas, Mant, Diakun & Nave, 1987), the peaks originate from the axial arrangements of myosin, C-protein and possibly titin/connectin in the thick filament (Malinchik & Lednev, 1992) and the assembly of the thin filaments containing actin, troponin, tropomyosin and possibly nebulin in the sarcomere (Squire, 1980). Protein arrangements in the two symmetrical halves of the thick and thin filaments across the *M* lines and *Z* bands (*e.g.* Craig, Alamo & Padron, 1992), respectively, diffract coherently to create numerous fine sampling peaks. The intensity tracings in Fig. 3 show that the peak-to-peak separation of the fine peaks sampling the thick-filament-based reflections is *ca* 700 nm and that of the peaks sampling the thin-filament-based reflections is *ca* 1000 nm. Fig. 3 also shows that a slightly different sampling pattern on the thick-filament-based meridional reflections is observed in the patterns from a frog sartorius (fast) muscle and a rat soleus (slow) muscle, indicating that the architecture of the thick filament is different in both types of skeletal muscles. Diffraction patterns of similarly high quality were also recorded from a mammalian fast muscle, showing a different pattern. Precise measurements of the peaks and comparison between different muscle types will enable us to elucidate the packing of protein molecules in the thick and thin filaments and also the arrangement of the thin and thick filaments in

the hexagonal lattice. A full account of the analysis will be presented after thorough model-building studies.

4.2. *Time-resolved experiments*

In time-resolved experiments the rotating-drum imaging-plate system (Amemiya *et al.*, 1988; Amemiya & Wakabayashi, 1991) was used as a one-dimensional detector. The drum rotated at 20 rotations s^{-1} and the circumference of the drum was 1080 mm. The vertical aperture of the entrance slit was set to 4 mm. The time resolution of this arrangement was 0.185 ms (50 ms × 4 mm/1080 mm). A small bundle of about ten fibers from chemically skinned rabbit *psoas* muscle was used in each experiment. The fiber bundle was oriented horizontally. The setting of the small muscle specimen in the beam was performed using a TV detector (Amemiya *et al.*, 1994) before starting each experiment. The length of the muscle bundle at almost full overlap between the thin and thick filaments in the sarcomere was oscillated at 500 Hz by a fast-moving servo motor synchronously with the rotation of the drum (Fig. 4). The peak-to-peak amplitude of oscillation was *ca* 0.6% of the muscle length (corresponding to ∼ 7 nm per half sarcomere). Thus, the drum circumference could accommodate the streak diffraction image of 25 complete 2 ms oscillations. In a typical total exposure time of 3 min, each of the 25 diffraction images represented the sum of the diffraction from 3600 oscillations. The oscillation diffraction patterns were read out as separate files and the
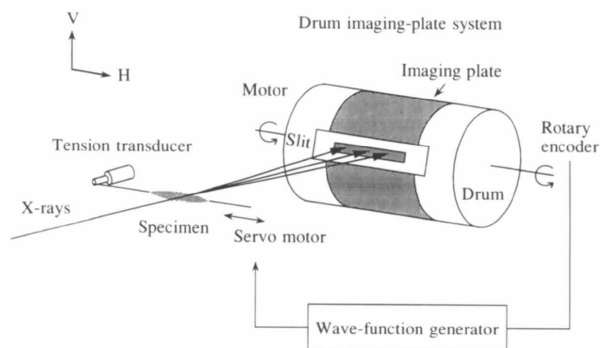

Figure 3
The intensity tracings on the meridian in the X-ray patterns from live skeletal muscles. The intensities are shown by multiplying the square of the axial coordinate for illustration purposes. Red line: from the frog sartorius (fast) muscle shown in Fig. 2. Green line: from a rat soleus (slow) muscle. *M*2–*M*10: thick-filament-based meridional reflections with a basic repeat of 43 nm in which *M*3 (the third order) is the 14.3 nm reflection. *C*: a 44 nm reflection from C-protein on the thick filaments. *TN*1–*TN*3: reflections with a repeat of 38 nm from troponin molecules on the thin filaments. All fine peaks come from sampling by the long-range periodicities in a sarcomere. The peak-to-peak separation of the fine peaks on the thick-filament-based reflections was *ca* 700 nm due to the sampling by the symmetrical halves of the thick filament across the *M* line in a sarcomere, and that of peaks on the troponin reflections was *ca* 1000 nm caused by interference from the assembly of the thin filaments across the *Z* bands.

25 images were summed to provide an averaged diffraction pattern with a high signal-to-noise ratio. Since a small fiber bundle diffracts X-rays weakly even with ca 10^{11} incident photons s^{-1} from the undulator beam, it was difficult to obtain fast time-resolved data on the weaker reflections and thus our measurement was restricted to only the 14.5 nm meridional reflection (indicated by an arrow in the case of a frog resting muscle in Fig. 2), one of the most intense in the pattern. Investigation of the intensity changes of this reflection is still informative. The experiments were performed at 281 K.

When small oscillatory length changes were applied to either active fibers or rigor fibers, the tension revealed a simple elastic response approximately in synchronism with length changes. Fig. 5 is a typical summed 2 ms-oscillation diffraction pattern from a bundle in a steady-state Ca^{2+}-activated contracting condition. Fig. 6 shows the results of a length change of the muscle fibers (a) and an intensity change of the 14.5 nm reflection (b) in one oscillation cycle. The intensity of the 14.5 nm reflection decreased during the stretching phase and increased during the releasing phase synchronously with the tension change. Similar results were obtained from fibers contracting in the presence of 20 mM inorganic phosphate (P_i) corresponding to a product of ATP hydrolysis. The obvious effect of P_i was to decrease the amount of tension change and the magnitude of the intensity change (data not shown). The addition of P_i was presumably to reduce the number of cross-bridges in strong binding states. In contrast, when the fibers were in a rigor state, strong oscillations occurred in the 14.5 nm intensity approximately in phase with the tension, *i.e.* increased tension during the stretch resulted in an increase in intensity of this reflection and *vice versa* (Fig. 6c). A control experiment using a relaxed bundle showed only very small oscillations in this reflection intensity, which can be attributed to variation in muscle thickness with stretch and release. In a rigor muscle the myosin heads are all firmly attached to actin in the same chemical state (which may correspond to the end of states in the ATP hydrolysis cycle) and in a relaxed muscle most of them are detached from actin. The present changes during high-frequency

Figure 4
The rotating-drum imaging system used for the time-resolved X-ray experiments during the length oscillation of the muscle fibers. An imaging plate (200 × 1000 mm) is attached on a rotating drum with a 1080 mm circumference. The drum rotated at a maximum speed of 20 rotations s^{-1}. A one-dimensional X-ray diffraction pattern which passes through the receiving slit is recorded on the imaging plate along the drum axis while intensity changes of the pattern as a function of time are recorded along the circumference. The vertical aperture of the entrance slit was 4 mm for the present experiments, so that the time resolution was 0.185 ms [rotation period (50 ms) × slit aperture (4 mm)/circumference (1080 mm)]. The length of the muscle fibers was oscillated at 500 Hz by a fast-moving servo motor in synchronism with the rotation of the drum using a rotary encoder. Tension changes were measured by a force transducer. The drum circumference accommodates the streak diffraction image of 25 complete 2 ms oscillations. After the exposure is finished, the streak image recorded on the imaging plate is read out with an He–Ne laser beam which scans the plate from behind the drum. The pixel size was 100 μm along the drum axis.
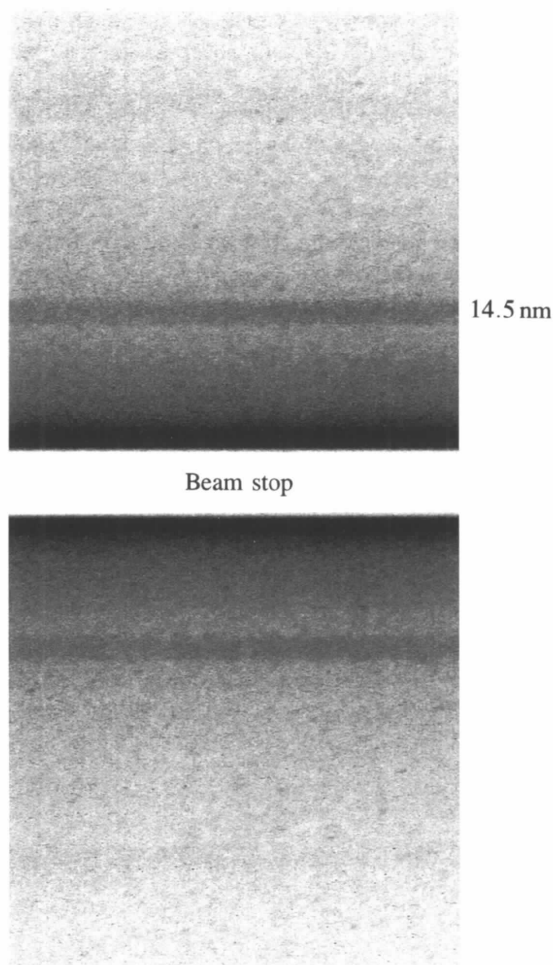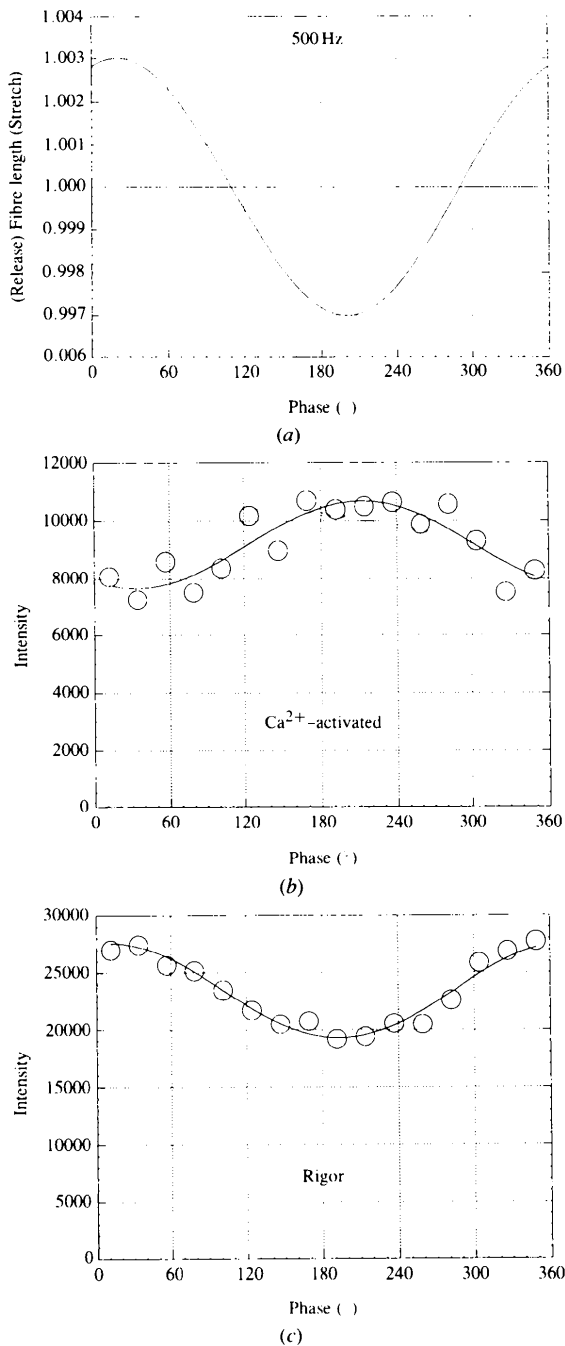

Figure 5
A typical example of the summed 2 ms-oscillation diffraction patterns from a muscle bundle (skinned rabbit *psoas*) during steady-state Ca^{2+}-activated contraction, recorded on an imaging plate on the drum. This streak diffraction image (25 complete 2 ms oscillations) represents the sum of the diffraction from 90 000 oscillations in a total exposure of typically 3 min. A 2 ms oscillation cycle corresponds to a length of 43.2 mm (432 pixels) on the imaging plate. The direction of rotation of the imaging plate is horizontal. The streak of the 14.5 nm reflection was marked and a faint streak of the second order of this reflection is seen.

oscillation (500 Hz) in active muscles were similar to those with rapid step-length changes (Lombardi *et al.*, 1995) but considerably different from the results with slow length oscillation (2–10 Hz) applied to the whole muscle during

Length change of the muscle fibers and intensity changes of the 14.5 nm meridional reflection in one oscillation cycle. The muscle bundle was oscillated at 500 Hz and with a peak-to-peak amplitude of 0.6% of the fiber length. [Tension changes occurred approximately in synchronism with the length changes (not shown).] (*a*) Oscillatory length change from either active fibers or rigor fibers, (*b*) a change of the 14.5 nm intensity in the active state, and (*c*) a change of the 14.5 nm intensity in rigor. In (*b*) and (*c*) the data points were taken from the sum of *ca* 90 000 individual oscillations in a total exposure.

isometric contraction (Mitsui *et al.*, 1994). In the case of rigor muscle, the changes were similar to those applied to a whole muscle in rigor (Tanaka, Wakabayashi & Amemiya, 1991). The different intensity response in active and rigor muscles provides useful information on the behavior of cross-bridges related to the force generation.

Although most of the myosin heads in an active muscle are at different stages of their working stroke, the application of rapid length oscillation to the muscle fibers may allow the partial synchronization of the movements of the myosin heads on a sub-millisecond timescale. The observed intensity changes of the 14.5 nm meridional reflection are likely to be due to an alteration of the projection of the mass of the population of myosin heads along the filament axis. These could be caused by a change in the conformation of the heads attached to the actin filaments. Since there is no net shortening during the oscillation, the structural change produced in the releasing phase must be reversed in the subsequent stretch phase. Assuming that the orientation of the head with a tadpole-like shape is somewhat off the perpendicular to the filament axis during the isometric state (Lombardi *et al.*, 1995), the intensity increase during the releasing phase could be accommodated by altering the orientation of the attached heads almost perpendicular to the fiber axis so that their mass projection is more sharply localized on the 14.5 nm plane. The intensity decrease during the stretching phase could be due to further tilting away from the isometric orientation, resulting in spreading out their mass projection along the filament axis. In rigor muscle fibers the intensity changes of this reflection were induced in the opposite direction to those observed in the active fibers. This reversal of the response could be explained if the average orientations of attached heads in the two states are on opposite sides of the plane perpendicular to the fiber axis (Irving *et al.*, 1995). Although such an explanation seems simple and plausible, it is premature to confine the intensity changes of this reflection solely to changes in the conformation of the attached heads. For a precise interpretation of the observed changes it would be necessary to consider various factors such as the two-headed nature of the myosin projection, interference of the diffraction from attached heads and free heads, possible detachment of heads from actin, and also elastic changes in the thick-filament backbone (Huxley, Stewart, Sosa & Irving, 1994; Wakabayashi *et al.*, 1994). Further analysis of the data will be required to assess quantitatively the magnitude of the intensity changes and find any phase shifts in intensity with respect to the imposed length change.

5. Conclusions

The results reported here demonstrate the usefulness of a highly collimated undulator beam from a third-generation storage ring. The most important features are low emittance and high flux. The advantage of the latter is obvious in high time-resolved experiments on small specimens. The former is also important, not only in a high-spatial-resolution study

like the one presented here but also in high time-resolved studies, because the low emittance beam allows the use of small optical elements (mirrors, monochromators) which function much more ideally than the large ones required by a wide beam from the usual bending magnet. The low emittance of an undulator source and these ideally functioning optics will create a well collimated beam that is suitable for experiments on small specimens with high resolution.

References

Amemiya, Y., Satow, Y., Matsushita, T., Chikawa, J., Wakabayashi, K. & Miyahara, J. (1988). *Top. Curr. Chem.* **226**, 353–367.

Amemiya, Y. & Wakabayashi, K. (1991). *Adv. Biophys.* **27**, 115–128.

Amemiya, Y., Wakabayashi, K., Hamanaka, T., Wakabayashi, T., Matsushita, T. & Hashizume, H. (1983). *Nucl. Instrum. Methods*, **208**, 471–477.

Amemiya, Y., Yagi, N., Kishimoto, S., Oguchi, T., Suzuki, M. & Wakabayashi, K. (1994). *Synchrotron Radiation in the Biosciences*, edited by B. Chance, J. Deisenhofer, S. Ebashi, D. T. Goodhead, J. R. Helliwell, H. E. Huxley, T. Iizuka, J. Kirz, T. Mitsui, E. Rubenstein, N. Sakabe, T. Sasaki, G. Schmahl, H. B. Stuhrmann, K. Wutrich & G. Zaccai, pp. 395–408. Oxford: Clarendon Press.

Ando, M. & Ohsumi, K. (1996). *Synchrotron Rad. News*. In the press.

Bordas, J., Mant, G. R., Diakun, G. P. & Nave, C. (1987). *J. Cell Biol.* **105**, 1311–1318.

Cooke, R. (1990). *Curr. Opin. Cell Biol.* **2**, 62–66.

Craig, R., Alamo, L. & Padron, R. (1992). *J. Mol. Biol.* **228**, 474–487.

Franks, A. (1958). *Br. J. Appl. Phys.* **9**, 349–352.

Holmes, K. C. (1974). *Endeavour*, **33**, 60–66.

Huxley, A. F. (1974). *J. Physiol (London)*, **243**, 1–43.

Huxley, H. E. & Brown, W. (1967). *J. Mol. Biol.* **30**, 383–434.

Huxley, H. E., Stewart, A., Sosa, H. & Irving, T. C. (1994). *Biophys. J.* **67**, 2411–2421.

Irving, M., Allen, T. S. C., Sabino-David, C., Craik, J. S., Brandmeier, B., Kendrick-Jones, J., Corrie, J. E. T., Trentham, D. R. & Goldman, Y. E. (1995). *Nature (London)*, **375**, 688–691.

Irving, T. C. & Huxley, H. E. (1994). *Synchrotron Radiation in the Biosciences*, edited by B. Chance, J. Deisenhofer, S. Ebashi, D. T. Goodhead, J. R. Helliwell, H. E. Huxley, T. Iizuka, J. Kirz, T. Mitsui, E. Rubenstein, N. Sakabe, T. Sasaki, G. Schmahl, H. B. Stuhrmann, K. Wutrich & G. Zaccai, pp. 519–529. Oxford: Clarendon Press.

Kamada, S., Fukuma, H., Ogata, A., Isawa, M., Nakamura, N., Sakanaka, S., Tobiyama, M., Kubo, T., Egawa, K., Mitsuhashi, T., Mimashi, T., Kobayashi, M. & Katsura, T. (1995). *Rev. Sci. Instrum.* **66**, 1913–1915.

Lombardi, V., Piazzesi, G., Ferenczi, M. A., Thirlwell, H., Dobble, I. & Irving, M. (1995). *Nature (London)*, **374**, 553–555.

Malinchik, S. B. & Lednev, V. V. (1992). *J. Muscle Res. Cell Motility*, **13**, 406–419.

Mitsui, T., Wakabayashi, K., Wang, En.-Z., Iwamoto, H., Tanaka, H., Kobayashi, T., Hamanaka, T., Amemiya, Y., Sugi, H., Ohshima, H. & Hiraoka, W. (1994). *Synchrotron Radiation in the Biosciences*, edited by B. Chance, J. Deisenhofer, S. Ebashi, D. T. Goodhead, J. R. Helliwell, H. E. Huxley, T. Iizuka, J. Kirz, T. Mitsui, E. Rubenstein, N. Sakabe, T. Sasaki, G. Schmahl, H. B. Stuhrmann, K. Wutrich & G. Zacca, pp. 460–472. Oxford: Clarendon Press.

Mori, T., Zhang, X., Sugiyama, H., Zhao, J., Ando, M. & Yoda, Y. (1995). *Rev. Sci. Instrum.* **66**, 2167–2170.

Rosenbaum, G., Holmes, K. C. & Witz, J. (1971). *Nature (London)*, **230**, 434–437.

Squire, J. (1980). *The Structural Basis of Muscular Contraction*. New York: Plenum Press.

Tanaka, H., Wakabayashi, K. & Amemiya, Y. (1991). *Adv. Biophys.* **27**, 105–113.

Tristan Super Light Facility Conceptual Design Report (1992). KEK Progress Report 92–1. KEK, Tsukuba, Japan.

Wakabayashi, K. & Amemiya, Y. (1990). *Handbook on Synchrotron Radiation*, Vol. 4, edited by S. Ebashi, M. Koch & E. Rubenstein, pp. 597–678. Amsterdam: Elsevier Science.

Wakabayashi, K., Sugimoto, Y., Tanaka, H., Ueno, Y., Takezawa, Y. & Amemiya, Y. (1994). *Biophys. J.* **67**, 2422–2435.

Yagi, N., Takemori, S. & Watanabe, M. (1993). *Adv. Exp. Med. Biol.* **332**, 423–432.

Yamamoto, S., Shioya, T., Kitamura, H. & Tsuchiya, K. (1995). *Rev. Sci. Instrum.* **66**, 1966–1968.